12th IFAC International Symposium on
Advanced Control of Chemical Processes
July 14-17, 2024. Toronto, Canada

Trajectory planning and tracking control for a one-stage spray dryer

A. Lepsien [*,**], **A. Schaum** [*,**]

[*] *Department of Process Analytics, University of Hohenheim, Stuttgart, Germany*
e-mail:{arthur.lepsien;alexander.schaum}@uni-hohenheim.de
[**] *Computational Science Hub, University of Hohenheim, Stuttgart, Germany*

Abstract: The present work deals with the control and observer design for a one–stage spray drying tower with focus on the optimization based trajectory planning and tracking control for an operation setpoint change during continuous operation. Putting emphasis on the numerical performance by employing different discretization schemes in combination with `CasADi`, key achievements are (i) an optimization-based system inversion for target trajectory generation, and (ii) a real-time capable model predictive tracking controller with computation times below one second in combination with either an extended Kalman Filter or a moving horizon estimator. The performance is shown in numerical simulations for a previously validated process model.

Keywords: Trajectory planning, tracking control, optimization, model predictive control, state estimation, `CasADi`

1. INTRODUCTION

As spray drying is a dominant process in process engineering of powdered products from liquids (Wrzosek et al., 2013), a big interest lies in its optimization (Petersen et al., 2017). The underlying physics can be formulated within a two-time scale system, where the thermodynamics evolve slowly with respect to the fast time-scale of the associated particle dynamics. Having as goal the achievement of a desired size distribution of the dried particles, the slow thermodynamic states are determined such that the product quality is ensured.

In previous control oriented works different Model Predictive Control (MPC) schemes are used to optimize and control a spray drying plant in continuous operation with the purpose to reject step disturbances in feed concentration or ambient humidity. In some cases a linear MPC with Real Time Optimization (RTO) is used (Petersen et al., 2014, 2015b) and the state estimation is done with a linear Kalman Filter. The goal in these works was to maximize the throughput and the residual moisture content while minimizing the supply of energy from the inlet air. Other works used an Economic Nonlinear MPC (Petersen et al., 2015a, 2017) in combination with an Extended Kalman Filter (EKF) based estimation scheme. In all these works, the sampling and computation time was set to $\Delta t = 30\,\mathrm{s}$. The authors mentioned, that future works should focus on speeding up the computational time, e.g. by employing `CasADi`.

Regarding the efficient implementation of schemes for continuous state estimation with discrete measurements, many studies have been reported so far. For the purpose of the present analysis the most important to mention are the works of (Boiroux et al., 2019; Frogerais et al., 2011; Kulikov and Kulikova, 2013) addressing the design of Continous Discrete Extended Kalman Filters (CDEKFs), and (Rao and Rawlings, 2000) proposing a solution using Moving Horizon Estimator (MHE), which in addition allows the consideration of inequality constraints on the states using dynamic programming.

The present work considers a different problem in regard to the spray drying operation, namely the change of operation setpoint of the spray drying unit during run–time. A possible scenario is, e.g., re-start up after a short power shortage or actuator failure. It is shown that by manipulation of the inlet flow of the liquid solution feed, the process variables can be steered back to the desired operation setpoint following an optimized trajectory for the thermodynamic states. Within this optimization step, it is possible to include constraints on the process variables, e.g. to prevent too low drying temperatures and condensation of water in the drying chamber. By an efficient use of different discretization schemes in combination with `CasADi`, it is shown that a trajectory tracking control using MPC in combination with an EKF or MHE based state estimation can be achieved within sampling times of $\Delta t = 1\,\mathrm{s}$, thus ensuring real–time capability with a normal PC. A comparison between the EKF and MHE based state estimation schemes for the considered spray drying process is provided in particular with regard to their measurement error compensation abilities.

2. PROBLEM DESCRIPTION

A typical spray dryer set up is shown in Figure 1, inspired by the Mini Büchi used for the validation of the model employed in the present study. The basic working principle is as follows. A bi–component solution of water and solvent is pumped by a peristaltic pump and it is atomized by

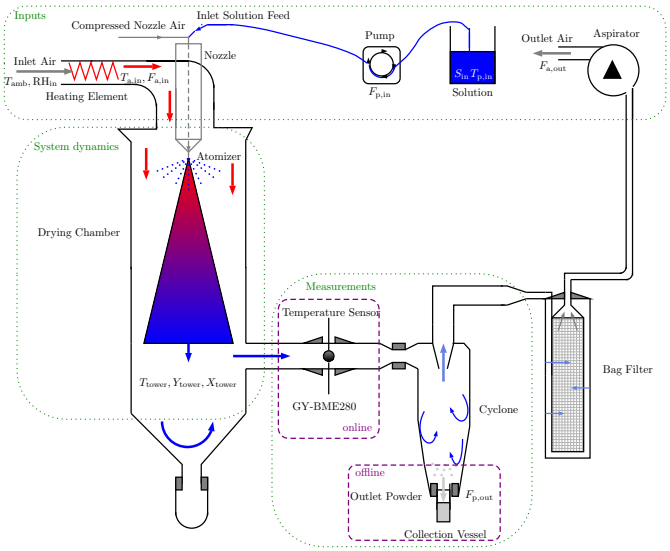

Fig. 1. Principle arrangement of a spray dryer, motivated by the case of the Mini Büchi B290, inspired by (Wrzosek et al., 2013).

the nozzle. The created droplets fall through the drying chamber within a concurrent flow field of air, the flow field is set by the aspirator volume flow. The air is heated by the inlet heating element. The dried particles are collected via the outlet cyclone. Too small particles find their way into the bag filter outlet.

The thermodynamic model of Lepsien and Schaum (2024) is used for optimization based trajectory planning and tracking. The coupled thermodynamic and particle dynamic model equations can be written in state space form as

$$\dot{\boldsymbol{x}} = \bar{\boldsymbol{f}}(\boldsymbol{x}, \boldsymbol{u}, p), \qquad t > 0, \quad \boldsymbol{x}(0) = \boldsymbol{x}_0 \tag{1a}$$
$$\boldsymbol{y} = \boldsymbol{h}(\boldsymbol{x}, \boldsymbol{u}), \tag{1b}$$
$$\epsilon \dot{p} = \mathcal{L}\left[\boldsymbol{x}, \boldsymbol{u}\right]\{p\}, \qquad t > 0, \quad p(0) = p_0 \tag{1c}$$
$$y_p = \bar{p}(\boldsymbol{x}, \boldsymbol{u}, s, t), \tag{1d}$$

where $\epsilon \ll 1$ represents the time scale variation and $\boldsymbol{x}(t) \in \mathbb{R}^n, \boldsymbol{u}(t) \in \mathbb{R}^p, \boldsymbol{y}(t) \in \mathbb{R}^m$ represent the thermodynamic state, input and output variables at time $t \geq 0$, respectively. The functions $\bar{\boldsymbol{f}} : \mathbb{R}^n_+ \times \mathbb{R}^p \times \mathcal{H} \to \mathbb{R}^n$ and $\boldsymbol{h} : \mathbb{R}^n_+ \to \mathbb{R}^m$ represent the thermodynamic dynamics with respect to both time scales. The operator $\mathcal{L}[\boldsymbol{x}, \boldsymbol{u}] : \mathcal{H} \to \mathcal{H}$ maps suitable function spaces $\mathcal{H}$ and is dependent on the thermodynamic system state. It describes the dynamics of the Particle Size Distribution (PSD) Probability Density Function (PDF) p, with associated measurement function $\bar{p}$, given, e.g., by the mean particle size, which most commonly is not available online.

For the purpose at hand, the specific dynamics of the PSD are neglected and approximated with noise entering the system model. The thermodynamic state variables of product X and air humidity Y as well as the tower temperature T are considered and summarized in the state vector $\boldsymbol{x} = [X_{\text{tower}}, Y_{\text{tower}}, T_{\text{tower}}]^{\text{T}}$. The detailed dynamics are elaborated in Lepsien and Schaum (2024) and summarized by

$$\dot{X}_{\text{tower}} = \frac{1}{m_{\text{s}}}\left[F_{\text{p,in}} X_{\text{in}} - F_{\text{p,out}} X_{\text{tower}} - R_{\text{w}}\right], \tag{2}$$

$$\dot{Y}_{\text{tower}} = \frac{1}{m_{\text{da}}}\Big[F_{\text{a,in}} Y_{\text{in}} - F_{\text{a,out}} Y_{\text{tower}} + \dots \\ R_{\text{w}} + F_{\text{add}} Y_{\text{add}} - F_{\text{add}} Y_{\text{tower}}\Big], \tag{3}$$

$$\dot{T}_{\text{tower}} = \frac{1}{C_{\text{thermal}}}\Big[F_{\text{a,in}} h_{\text{a,in}} - F_{\text{a,out}} h_{\text{a,out}} + \\ F_{\text{p,in}} h_{\text{p,in}} - F_{\text{p,out}} h_{\text{p,out}} - Q_{\text{evap}} - Q_{\text{loss}} \\ - F_{\text{add}} h_{\text{a,out}} + F_{\text{add}} h_{\text{a,add}}(T_{\text{tower}})\Big], \tag{4}$$

with $F_{\text{a,in}}, F_{\text{a,out}}$ being the inlet and outlet air mass flows, and $F_{\text{p,in}}, F_{\text{p,out}}$ the inlet and outlet solution mass flows. The values of these quantities are determined by the functions

$$F_{\text{a,in}} = \dot{v}_{\text{a,in}} \rho_{\text{a,in}} = \dot{v}_{\text{a,in}} \frac{M_{\text{a,in}} P_0}{R T_{\text{a,in}}}, \tag{5}$$

$$F_{\text{a,out}} = \dot{v}_{\text{a,out}} \rho_{\text{a,out}} = \dot{v}_{\text{a,out}} \frac{M_{\text{a,out}} P_0}{R T_{\text{tower}}}, \tag{6}$$

$$F_{\text{p,in}} = \dot{v}_{\text{p,in}} \left(\rho_{\text{s}} S_{\text{in}} + \rho_{\text{w}} \left[1 - S_{\text{in}}\right]\right), \tag{7}$$

$$F_{\text{p,out}} = \dot{v}_{\text{p,out}} \left(\rho_{\text{s}} S_{\text{tower}} + \rho_{\text{w}} \left[1 - S_{\text{tower}}\right]\right), \tag{8}$$

with

$$\dot{v}_{\text{p,in}} = \dot{v}_{\text{pump}}, \qquad \dot{v}_{\text{p,out}} = \dot{v}_{\text{pump}} - \frac{R_{\text{w}}}{\rho_{\text{w}}}, \tag{9}$$

$$\dot{v}_{\text{a,in}} = \dot{v}_{\text{aspirator}} - \frac{R_{\text{w}}}{\rho_{\text{v}}}, \quad \dot{v}_{\text{a,out}} = \dot{v}_{\text{aspirator}}, \tag{10}$$

where the water evaporation rate R_{w} corrects the volume intake of air $\dot{v}_{\text{a,in}}$ and the powder outtake $\dot{v}_{\text{p,out}}$ by their corresponding set values of the process control unit. The specific equations for the evaporation rate and equilibrium moisture content can be found in Lepsien and Schaum (2024). Additionally, the relative humidity is measured with the measurement function

$$\text{RH}(T, Y) = \frac{Y}{\frac{M_{\text{v}}}{M_{\text{da}}} + Y} \frac{P_0}{P_{\text{v}}^{\text{sat}}(T)}, \tag{11}$$

with the saturation pressure $[P_{\text{v}}^{\text{sat}}] = \text{Pa}$ described in (Smith et al., 2018) and the atmospheric pressure P_0.

In this work, as control input only the inlet flow of the liquid solution feed $\dot{v}_{\text{pump}}$ is considered. Therefore, the inlet temperature, outflow velocity (fixed by the aspirator) and liquid composition are considered constant. Furthermore, the process is typically subject to fluctuations and the measurement is subject to noise. These considerations lead to a stochastically perturbed input affine system of the form

$$\dot{\boldsymbol{x}} = \boldsymbol{f}(\boldsymbol{x}) + \boldsymbol{g}(\boldsymbol{x}) u + \boldsymbol{w}, \quad t > 0, \quad \boldsymbol{x}(0) = \boldsymbol{x}_0, \tag{12a}$$
$$\boldsymbol{y}_k = \boldsymbol{h}(\boldsymbol{x}_k) + \boldsymbol{v}_k, \qquad t \geq 0, \tag{12b}$$

with $\boldsymbol{f}, \boldsymbol{g}$ chosen according to (2)-(4), and the discrete measurement function $\boldsymbol{h}(\boldsymbol{x}_k) = [\text{RH}\ T]^T$,. Additionally the disturbances in the system are described by $\boldsymbol{w} \sim \mathcal{N}(0, Q)$ and $\boldsymbol{v} \sim \mathcal{N}(0, R)$ representing a zero mean multivariate Gaussian process and measurement noise, respectively.

3. TRAJECTORY PLANNING

The idea behind the trajectory planning is, in case of power failure and process plant shut–down, the system should be brought into the desired operation point in the fastest and most cost–efficient way as possible. For this purpose, first

the actual state needs to be determined and then a suitable trajectory needs to be determined along which the states can be steered back to the desired operation setpoint.

The trajectory planning problem can be formulated as an Optimal Control Problem (OCP) which aims to find an optimal control input $u^*(t)$ that drives the system from an initial state $\boldsymbol{x}_0$ to a desired final state $\boldsymbol{x}_\mathrm{f}$ within prescribed bounds on the system input and states, while minimizing the cost functional J with

$$\begin{aligned} \min_{u} \quad & J^p(u) := \int_{t_0}^{t_f} L^\mathrm{p}(\boldsymbol{x}(t), u(t), t)dt \\ \text{subject to} \quad & \dot{\boldsymbol{x}} = \boldsymbol{f}(\boldsymbol{x}) + \boldsymbol{g}(\boldsymbol{x})u \\ & \boldsymbol{x}(t_0) = \boldsymbol{x}_0, \quad \boldsymbol{x}(t_\mathrm{f}) = \boldsymbol{x}_\mathrm{f} \\ & u_\mathrm{min} \leq u(t) \leq u_\mathrm{max}, \quad \boldsymbol{x} \in X \end{aligned} \tag{13}$$

where t_0 and t_f are the initial and final times, u_min and u_max are the lower and upper bounds on the control input, and $X \subset \mathbb{R}^3_+$ is a suitable polytope satisfying physical and safety constraints on the states. The Langrangian $L^p(\boldsymbol{x}(t), u(t), t)$ is the instantaneous cost function at time t, which penalizes deviations from desired behavior and may include control effort, state errors, or other relevant measures, such as economic considerations. In this work the cost function is constructed from the state deviation from the target value $\boldsymbol{x}_\mathrm{f}$, the input value, which also reflects the cost of the process, and the derivative of the input variable leading to

$$\begin{aligned} L^\mathrm{p} = & \left[\boldsymbol{x}(t) - \boldsymbol{x}_\mathrm{f}\right]^\mathrm{T} V^\mathrm{p} \left[\boldsymbol{x}(t) - \boldsymbol{x}_\mathrm{f}\right] \\ & + W^\mathrm{p} u^2(t) + S^\mathrm{p} \dot{u}^2(t). \end{aligned} \tag{14}$$

Solving the optimization-based trajectory planning problem can involve various numerical optimization techniques, such as gradient-based methods, direct transcription methods, or evolutionary algorithms. Efficient algorithms and software tools are available to handle complex systems and high-dimensional control inputs. In this paper, multiple shooting within `CasADi`(Andersson et al., 2019) is employed. It should be noted that this is the first time this approach is used to study the considered problem as to the authors knowledge.

By applying multiple shooting, the OCP is transformed into a finite-dimensional Nonlinear Program (NLP). The obtained optimal control sequence $\boldsymbol{U}^\mathrm{p} = [u_0^\mathrm{p}, u_1^\mathrm{p}, \ldots, u_{M-1}^\mathrm{p}]$ can then be applied to the system.

The time derivative approximation of the input is given by $\dot{u} \approx \frac{1}{\Delta t}(u_k - u_{k-1})$. Afterwards, the cost function is set up to be

$$\begin{aligned} J_\mathrm{d}^\mathrm{p}(\boldsymbol{U}^\mathrm{p}) = & \sum_{k=0}^{M-1} \left[\boldsymbol{x}_k^\mathrm{p} - \boldsymbol{x}_\mathrm{f}\right]^\mathrm{T} V^\mathrm{p} \left[\boldsymbol{x}_k^\mathrm{p} - \boldsymbol{x}_\mathrm{f}\right] \\ & + W^\mathrm{p} \left(u_k^\mathrm{p}\right)^2 + S^\mathrm{p} \left(u_k^\mathrm{p} - u_{k-1}^\mathrm{p}\right)^2. \end{aligned} \tag{15}$$

Between each interval of size Δt, a system shift occurs, representing the solution of the system Ordinary Differential Equation (ODE), that can be computed with different discretization schemes. The discretization scheme found to be the most effective for this trajectory planning problem is the implicit Euler method, since the step size can be chosen relatively large. The usage of the implicit Euler scheme is interesting for the trajectory planning approach, as the convergence will not depend on the choice of the number of time intervals M. Due to this advantage, the dimensionality of the multiple shooting OCP can be reduced and a faster computation follows. The disadvantage of this approach in the context of input planning, is that at t_f the input for the next time instant has to be known. In this work, this problem is surpassed, by setting $u_{N+1} = u_N$ in the planning. This approach is useful in the case of spray drying as a flow of solution into the drying unit is necessary for the drying operation.

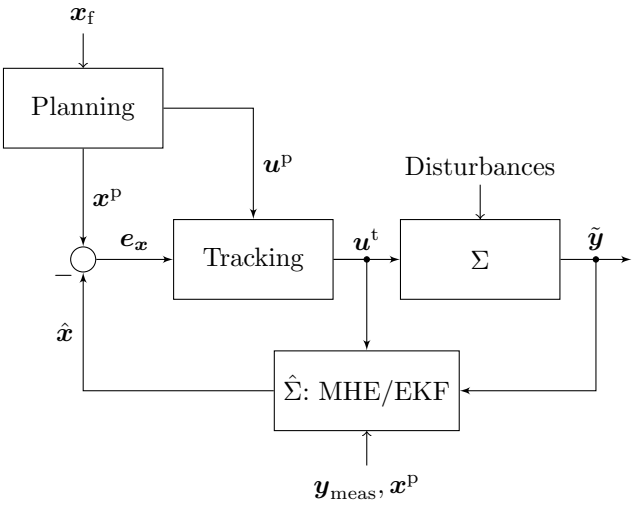

Fig. 2. Block diagram of the trajectory tracking problem.

4. TRAJECTORY TRACKING

The schematic diagram of the tracking control scheme can be seen in Fig. 2. To track the planned state trajectory $\boldsymbol{x}^\mathrm{p}(t)$, an MPC is used.

4.1 MPC

The objective of the model predictive tracking control is to find the optimal control sequence $\boldsymbol{U}^\mathrm{t} = [u_0^\mathrm{t}, u_1^\mathrm{t}, \ldots, u_{M-1}^\mathrm{t}]$ that minimizes the cost function

$$\begin{aligned} J_\mathrm{d}^\mathrm{t}(\boldsymbol{U}^\mathrm{t}) = & \sum_{k=0}^{M-1} \left[\boldsymbol{x}_k^\mathrm{p} - \boldsymbol{x}_k^\mathrm{t}\right]^\mathrm{T} V^\mathrm{t} \left[\boldsymbol{x}_k^\mathrm{p} - \boldsymbol{x}_k^\mathrm{t}\right] \\ & + W^\mathrm{t} \left(u_k^\mathrm{p} - u_k^\mathrm{t}\right)^2 + S^\mathrm{t} \left(u_k^\mathrm{t} - u_{k-1}^\mathrm{t}\right)^2, \end{aligned} \tag{16}$$

subject to input and state constraints, similarly to the planning.

While the MPC is similar to the planning problem there are two main differences. First, in the cost function the deviations from the planned state and input trajectories are considered instead of the reference values. Secondly, Runge-Kutta of order 4 is employed to calculate the state shift, with constant inputs u_k between sampling intervals. The reason for the different choice of discretization is that the differential equation can behave stiffly over the planning horizon and therefore an implicit method provides more robust results. A small horizon is used for the tracking controller and therefore an explicit method can be used. Again, an efficient solution of this optimization problem is achieved using `CasADi`.

4.2 Nonlinear state estimation

As can be seen in the optimization problem cost function (16) the tracking state $\boldsymbol{x}^t$ needs to be known in each sampling point. As only parts of the state vector $\boldsymbol{x}$ are measured it is necessary to implement a state estimation scheme. In the following, two different observers are compared, namely the MHE and EKF. They are designed and employed in this paper to estimate the system state, which is necessary to set up the trajectory tracking problem.

MHE The MHE, also known as Nonlinear Model Predictive Estimation (NMPE), is an advanced state estimation technique used to estimate the states of a dynamic system using a sequence of measurements over a moving time horizon (Sun et al., 2014; Hedengren et al., 2014).

The MHE estimation problem can be formulated as a sequential optimization problem. At each time step k, we define a moving time horizon N that contains the most recent N measurements. The objective is to find the state estimate $\hat{\boldsymbol{x}}_k$ that minimizes a cost function over the preceding horizon N and reads

$$\hat{\boldsymbol{x}}_k = \underset{x_{k-N},\ldots,x_k}{\operatorname{argmin}} \; J_{\mathrm{d}}^{\mathrm{MHE}} \tag{17}$$

$$J_{\mathrm{d}}^{\mathrm{MHE}} = \sum_{i=0}^{N} (\boldsymbol{y}_{k-i} - \boldsymbol{h}(\hat{\boldsymbol{x}}_{k-i}))^{\mathrm{T}} \, R^{-1} (\boldsymbol{y}_{k-i} - \boldsymbol{h}(\hat{\boldsymbol{x}}_{k-i}))$$

with the inverse measurement noise covariance R^{-1}. It would also be possible to include the input estimation due to actuator inaccuracies with the term $(u_{k-i} - \hat{u}_{k-i})^2 T^{-1}$, containing the inverse actuator error covariance T^{-1}. The summation is performed over the preceding horizon of N steps. The optimization problem is subject to the state dynamics and control constraints to ensure the feasibility of the estimated state trajectory. The MHE algorithm can be cast into a NLP formulation similarly as above described. For the solution `CasADi` is employed, as well.

EKF For comparison, an EKF is implemented and compared with the above MHE observer. The observer implemented in regard to the system at hand, is a CDEKF, as described in (Boiroux et al., 2019; Frogerais et al., 2011; Kulikov and Kulikova, 2013) with regular sampling points at $t_k = k\Delta t$. Here, the sampling time $\Delta t = 1\,\mathrm{s}$. The main idea consists in using the actual estimate $\hat{\boldsymbol{x}}(t_k)$ at time t_k as initial value for obtaining a state estimate $\hat{\boldsymbol{x}}(t)$ for $t \in [t_k, t_{k+1})$ according to

$$\dot{\hat{\boldsymbol{x}}}_{\mathrm{p}} = \boldsymbol{f}(\hat{\boldsymbol{x}}_{\mathrm{p}}) + \boldsymbol{g}(\hat{\boldsymbol{x}}_{\mathrm{p}})u, \quad t \in (t_k, t_{k+1}], \tag{18}$$

with initial condition $\hat{\boldsymbol{x}}_{\mathrm{p}}(t_k) = \hat{\boldsymbol{x}}(t_k)$, and the associated covariance prediction according to

$$\dot{P}_{\mathrm{p}} = A_k P_{\mathrm{p}} + P_{\mathrm{p}} A_k^{\mathrm{T}} + Q, \quad t \in (t_k, t_{k+1}], \tag{19}$$

with initial condition $P_{\mathrm{p}}(t_k) = P(t_k)$. These ODEs are solved with `ode15s` in MATLAB. The jacobians A and C are given by

$$A_k = \frac{\partial \boldsymbol{f}}{\partial \boldsymbol{x}}(\hat{\boldsymbol{x}}(t_k)) + \frac{\partial \boldsymbol{g}}{\partial \boldsymbol{x}}(\hat{\boldsymbol{x}}(t_k))\boldsymbol{u}(t_k), \quad C_k = \frac{\partial \boldsymbol{h}}{\partial \boldsymbol{x}}(\hat{\boldsymbol{x}}(t_k)).$$

Corrections take place at the sampling instants t_k only, according to

$$\hat{\boldsymbol{x}}(t_{k+1}) = \hat{\boldsymbol{x}}_{\mathrm{p}}(t_{k+1}) + L_{k+1} \left(\boldsymbol{y} - \boldsymbol{h}(\hat{\boldsymbol{x}}_{\mathrm{p}}(t_{k+1})) \right), \tag{20}$$

$$P_{k+1} = (I - L_{k+1} C_{k+1}) \, P_{\mathrm{p}}. \tag{21}$$

with the correction gain L_{k+1} being given by

$$L_{k+1} = P_{\mathrm{p}} C_{k+1}^{\mathrm{T}} \left(C_{k+1} P_{\mathrm{p}} C_{k+1}^{\mathrm{T}} + R \right)^{-1}. \tag{22}$$

5. CASE STUDY

As a case study, the constant input variables in (1a) are set. The outlet aspirator air flow is set to $\dot{v}_{\mathrm{a}} = 35\,\mathrm{m^3\,h^{-1}}$, the inlet powder concentration to $S_{\mathrm{in}} = 10\,\%$ and the inlet heated air temperature to $T_{\mathrm{a,in}} = 135\,^{\circ}\mathrm{C}$. This case study uses $V^{\mathrm{p}} = \mathrm{diag}\left[1 \cdot 10^4, 1 \cdot 10^4, 1 \cdot 10^0\right]$, $W^{\mathrm{p}} = 1 \cdot 10^{-2}$ and $S^{\mathrm{p}} = 1 \cdot 10^1$ for the planning cost function and $V^{\mathrm{t}} = \mathrm{diag}\left[1 \cdot 10^4, 1 \cdot 10^4, 1 \cdot 10^0\right]$, $W^{\mathrm{t}} = 1 \cdot 10^{-2}$, $R_{\mathrm{undis.}} = \mathrm{diag}\left[1 \cdot 10^{-4}, 5 \cdot 10^{-10}\right]$, $R_{\mathrm{dis.}} = \mathrm{diag}\left[5 \cdot 10^{-1}, 5 \cdot 10^{-5}\right]$ and $Q = \mathrm{diag}\left[1 \cdot 10^{-6}, 1 \cdot 10^{-9}, 1 \cdot 10^{-5}\right]$ in the tracking cost function.

To compare these observers, different scenarios are simulated. Firstly, one with very little noise on the measurements without input disturbances. Secondly, more significant noise on the measurements without input disturbances. It should be noted, that the MHE only starts to correct the state prediction with the measurements after N time steps, whereas the EKF starts the prediction immediately. Note, that due to the implementation of the MHE, in the first steps, until the moving horizon of the estimator is filled with measurements, the planned control inputs are used and the tracking MPC starts to optimize, when the MHE starts to give a state estimate. In this implementation, the MPC horizon is chosen as $M = 10$ and the MHE horizon as $N = 10$, respectively. The control action is computed for every time step. Furthermore, it was necessary to change the cost function for the MHE based MPC, such that the input derivative is penalized harder in the case, when noise is present in the system. If this would not be done, the solver does not converge. The EKF based MPC would have converged for lower input derivative penalty, but for comparability the value is chosen equally for both approaches to be $S^{\mathrm{t}} = 1 \cdot 10^5$. It should be noted, that the initial condition of the observers is set to be the same as in the simulated system, as the trajectory planning works with this initial condition.

To ensure real–time capability of the system, a simulation with 600 time steps is conducted ten times with the same random seed for all simulations and the time of each optimization step is calculated. The corresponding statistics can be found in Tab. 1. The standard IPOPT Wächter and Biegler (2006) options are used in `CasADi`. Note, that all solver times are below the sampling interval of $\Delta t = 1\,\mathrm{s}$, the maximum times for the MHE occur at the first estimation step. The reason behind this can be the initialization of the MHE with the planned input trajectory and the disturbed system states. It should be noted, that the EKF based approach seems more suitable, as the estimator is deterministic in computational time and has a lower mean and maximum MPC step time than the optimization based MHE scheme. In any case, if the computational time would exceed the sampling time, the MPC control input for this instance can be chosen, as it plans with M steps into the future at the given time instance.

Table 1. Solver time statistics for the disturbed systems in seconds.

Context	Component	Value
MPC–EKF	t_{mean}	0.0197
	t_{median}	0.0187
	t_{max}	0.1882
	t_{min}	0.0180
MPC–MHE	t_{mean}	0.0397
	t_{median}	0.0371
	t_{max}	0.9846
	t_{min}	0.0328

The planning and tracking input results can be found in Fig. 3 for the disturbed system. The simulated state

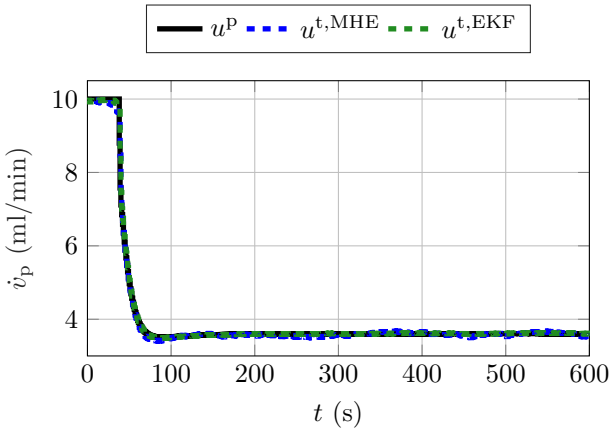

Fig. 3. Input Trajectories in the disturbed simulation.

trajectories in state space can be found in Fig. 4 for the disturbed case. Additionally, the resulting state evolution

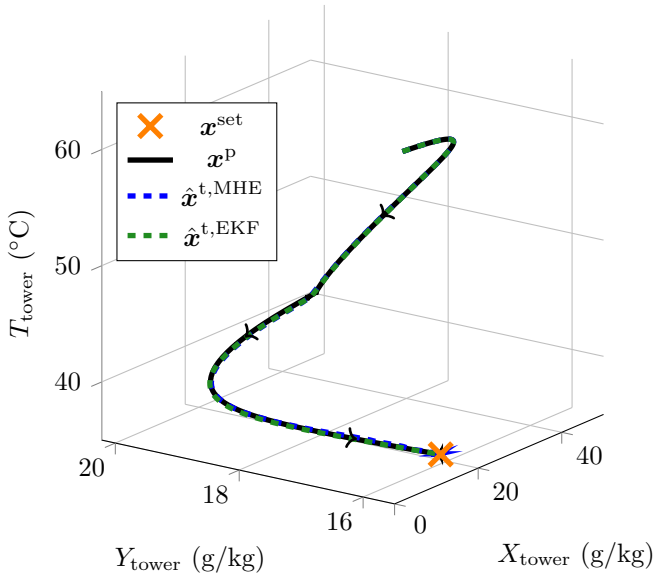

Fig. 4. Resulting state vector $\boldsymbol{x}(t)$ in phase space from the closed–loop simulation with the planned input of the planning MPC, the set-point is marked as an orange cross, estimated trajectories are dashed.

of the disturbed system over time can be seen in Fig. 5 and the corresponding disturbed measurements used for state estimation can be found in Fig. 6.

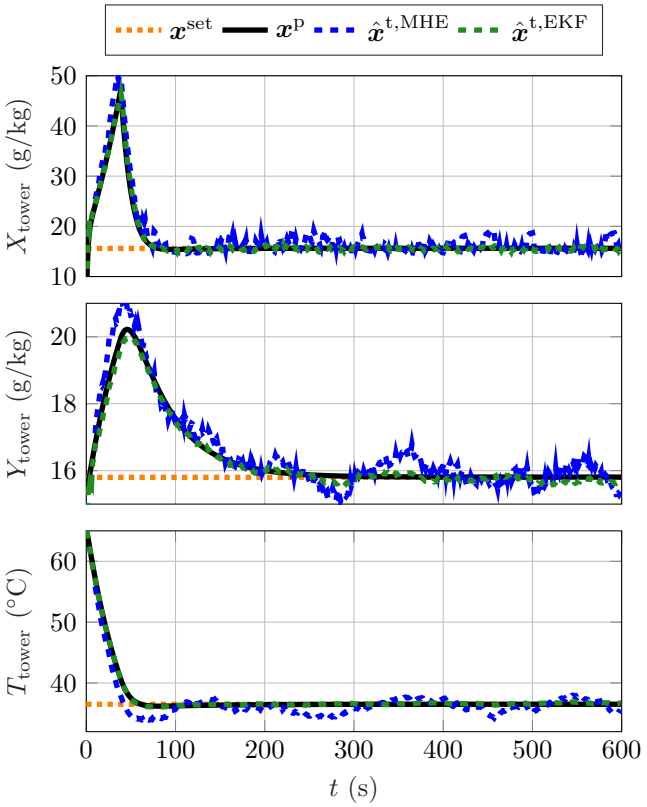

Fig. 5. Resulting state vector $\boldsymbol{x}(t)$ from the closed–loop simulation with measurement noise and comparison between both estimator types.

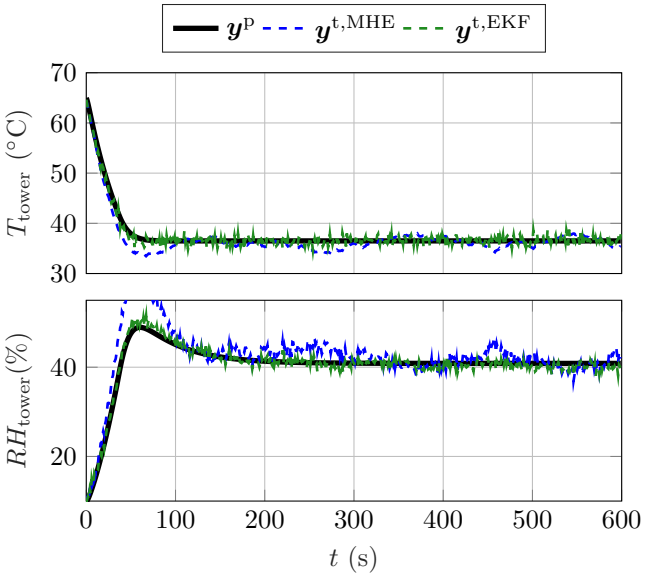

Fig. 6. Disturbed measurements of both estimation schemes.

6. CONCLUSION

In this paper a MPC for the slow manifold of a spray drying operation in combination with two different estimation schemes is designed and tested numerically. It is shown, that trajectory planning and tracking with the combined controller–estimator schemes work, even if noise is entering the system. Furthermore, it is shown, that the

usage of `CasADi` speeds up the computational time, to ensure real–time applicability with an one second actuator time interval. A future research problem is the change of the set-point trajectory planning to another optimization problem, which couples the particle- and thermodynamics. Solving this optimization problem will again result in a thermodynamic trajectory to be tracked with an MPC. Here, particle distribution measurements could also be included into the estimator model to achieve a better convergence of the controller.

REFERENCES

Andersson, J.A.E., Gillis, J., Horn, G., Rawlings, J.B., and Diehl, M. (2019). CasADi – A software framework for nonlinear optimization and optimal control. Mathematical Programming Computation, 11(1), 1–36. doi:10.1007/s12532-018-0139-4.

Boiroux, D., Ritschel, T.K., Poulsen, N.K., Madsen, H., and Jørgensen, J.B. (2019). Efficient computation of the continuous-discrete extended kalman filter sensitivities applied to maximum likelihood estimation. In 2019 IEEE 58th Conference on Decision and Control (CDC), 6983–6988. IEEE.

Frogerais, P., Bellanger, J.J., and Senhadji, L. (2011). Various ways to compute the continuous-discrete extended kalman filter. IEEE Transactions on Automatic Control, 57(4), 1000–1004.

Hedengren, J.D., Shishavan, R.A., Powell, K.M., and Edgar, T.F. (2014). Nonlinear modeling, estimation and predictive control in apmonitor. Computers & Chemical Engineering, 70, 133–148.

Kulikov, G.Y. and Kulikova, M.V. (2013). Accurate numerical implementation of the continuous-discrete extended kalman filter. IEEE Transactions on Automatic Control, 59(1), 273–279.

Lepsien, A. and Schaum, A. (2024). Thermodynamic model identification for a one-stage spray dryer. IFAC-PapersOnLine, accepted (IFAC AdChem2024).

Petersen, L.N., Jørgensen, J.B., and Rawlings, J.B. (2015a). Economic optimization of spray dryer operation using nonlinear model predictive control with state estimation. IFAC-PapersOnLine, 48, 507–513.

Petersen, L.N., Poulsen, N.K., Niemann, H.H., Utzen, C., and Jørgensen, J.B. (2014). Application of constrained linear mpc to a spray dryer. In 2014 IEEE Conference on Control Applications (CCA), 2120–2126. IEEE.

Petersen, L.N., Poulsen, N.K., Niemann, H.H., Utzen, C., and Jørgensen, J.B. (2015b). Comparison of linear and nonlinear model predictive control for optimization of spray dryer operation. IFAC-PapersOnLine, 48(23), 218–223.

Petersen, L.N., Poulsen, N.K., Niemann, H.H., Utzen, C., and Jørgensen, J.B. (2017). Comparison of three control strategies for optimization of spray dryer operation. Journal of Process Control, 57, 1–14.

Rao, C.V. and Rawlings, J.B. (2000). Nonlinear moving horizon state estimation. In Nonlinear model predictive control, 45–69. Springer.

Smith, J., Van Ness, H., and Abbott, M. (2018). Introduction to Chemical Engineering Thermodynamics. CHEMICAL ENGINEERING SERIES. McGraw-Hill Education.

Sun, L., Hedengren, J.D., and Beard, R.W. (2014). Optimal trajectory generation using model predictive control for aerially towed cable systems. Journal of Guidance, Control, and Dynamics, 37(2), 525–539.

Wächter, A. and Biegler, L.T. (2006). On the implementation of an interior-point filter line-search algorithm for large-scale nonlinear programming. Mathematical programming, 106, 25–57.

Wrzosek, K., Moravčík, J., Antošová, M., Illeová, V., and Polakovič, M. (2013). Spray drying of the mixtures of mono-, di-, and oligosaccharides. Acta Chimica Slovaca, 6(2), 177–181.

Appendix A. PARAMETER TABLES

Table A.1. Simulation Parameters.

Context	Constant	Value	Unit
Fixed Parameters			
Density	ρ_{s}	1.514	$\mathrm{g\,mL^{-1}}$
	ρ_{w}	1.0	$\mathrm{g\,mL^{-1}}$
Molar Mass	M_{da}	28.9647	$\mathrm{g\,mol^{-1}}$
	M_{v}	18.01528	$\mathrm{g\,mol^{-1}}$
	M_{w}	18.01528	$\mathrm{g\,mol^{-1}}$
Gas Constant	R	8.3145	$\mathrm{J\,mol^{-1}\,K^{-1}}$
Antoine Equation	A	16.3872	–
	B	3885.7	°C
	C	230.17	°C
Heat Capacity Dry Air	A_{da}	3.355	–
	B_{da}	$0.575 \cdot 10^{-3}$	$\mathrm{K^{-1}}$
	C_{da}	0	$\mathrm{K^{-2}}$
	D_{da}	$-0.016 \cdot 10^{5}$	$\mathrm{K^{2}}$
Heat Capacity Water Vapor	A_{v}	3.470	–
	B_{v}	$1.450 \cdot 10^{-3}$	$\mathrm{K^{-1}}$
	C_{v}	0	$\mathrm{K^{-2}}$
	D_{v}	$0.121 \cdot 10^{5}$	$\mathrm{K^{2}}$
Heat Capacity Liquid Water	A_{w}	8.712	–
	B_{w}	$1.25 \cdot 10^{-3}$	$\mathrm{K^{-1}}$
	C_{w}	$-0.18 \cdot 10^{-6}$	$\mathrm{K^{-2}}$
	D_{w}	0	$\mathrm{K^{2}}$
Latent Heat	λ_{ref}	2257	$\mathrm{J\,g^{-1}}$
	$T_{\mathrm{ref,evap}}$	373.15	K
	α	647.1	K
	β	0.38	–
Thin-Layer Equation	T_0	298.15	K
Heat Capacity Solid Mannitol	$A_{\mathrm{s,m}}$	207.790	–
	$B_{\mathrm{s,m}}$	141.210	–
	$C_{\mathrm{s,m}}$	−23.623	–
	$D_{\mathrm{s,m}}$	−38.543	–
	$E_{\mathrm{s,m}}$	44.992	–
	$F_{\mathrm{s,m}}$	23.902	–
	$G_{\mathrm{s,m}}$	−32.126	–
	T_{min}	90	K
	T_{max}	390	K
Identified Parameters			
Masses	m_{s}	0.1	kg
	m_{da}	6	kg
Thin-Layer Equation	$k_{\mathrm{w},1}$	$3 \cdot 10^{-2}$	$\mathrm{s^{-1}}$
	$k_{\mathrm{w},2}$	$2.50 \cdot 10^{4}$	$\mathrm{J\,mol^{-1}}$
	$k_{\mathrm{w},3}$	0.10016	–
GAB	X_0'	0.2759	$\mathrm{kg\,kg^{-1}}$
	K'	0.8987	$\mathrm{kg\,kg^{-1}}$
	C'	0.2221	$\mathrm{kg\,kg^{-1}}$
	ΔH_X	500	$\mathrm{J\,mol^{-1}}$
	ΔH_K	500	$\mathrm{J\,mol^{-1}}$
	ΔH_C	500	$\mathrm{J\,mol^{-1}}$
	X_{add}	$-7.804 \cdot 10^{-5}$	$\mathrm{kg\,kg^{-1}}$
Heat Loss	k_{UA}	0.0899	$\mathrm{W\,K^{-1}}$
Heat Capacity	C_{thermal}	$9 \cdot 10^{3}$	$\mathrm{J\,K^{-1}}$
Additive Parts	Y_{add}	0.0117	$\mathrm{kg\,kg^{-1}}$
	T_{add}	320.5	K
	F_{add}	0.11	$\mathrm{kg\,s^{-1}}$